Formalism of Dielectric Function and Depolarization in SWNT: Application to Nano–Optical Switches and Probes

Slava V. Rotkin

Beckman Institute for Advanced Science and Technology,
University of Illinois at Urbana–Champaign,
405 N.Mathews, Urbana, IL 61801, USA

ABSTRACT

The paper reviews current theoretical methods to study quasi–electrostatic phenomena in single–wall nanotube systems. Several models are presented to demonstrate importance of selfconsistent calculation of the electric fields for electronic device applications. The quantum mechanical formalism of the dielectric function is chosen to obtain the selfconsistent solution. It gives a unified approach to calculate exciton binding energy, to obtain transverse and longitudinal polarization in the nanotube, to study symmetry breaking and band gap engineering in electric fields, and to perform modelling of ballistic transport in a light–operated switches.

Keywords: nanotube, theory, dielectric function formalism, nanodevices, depolarization, nano–optics, band-structure, band gap engineering, molecular switch, near–field optics

1. INTRODUCTION

Nanotubes, scrolled concentric cylinders of graphite, are in focus of attention of scientists and engineers already for 13+ years. Since the discovery in 1991,[1] these one–dimensional (1D) nanostructures showed deep physics, promising chemistry and found numerous applications. Among most interesting are field emission applications, use for mechanical strengthening components and electronic applications. The field of optics of nanotubes is still at an early stage both in experiment and theory.

Optics of semiconductors and semiconductor nanostructures essentially bases of the fundamentals of theory established in early 60–ies when the success of many body methods allowed quantum mechanical derivation of the dielectric function. Since that time the formalism of dielectric function, which was used as a phenomenological theoretical method for a while, became the powerful tool for predicting optical effects. We found that the nanotube systems, and especially single–wall nanotubes, have some specifics that make using textbook formulas difficult if even possible. Though, a complete quantum mechanical theory of an effective dielectric function of a nanotube is not developed, we report here on several interesting aspects of this study.

It was published recently, that nanotubes may be used for near–field optical microscope (NSOM) tips.[2,3] Due to almost atomic sharpness of the nanotube tip it may serve to obtain super–high resolution in non–destructive optical imaging. We model the response of the single–wall nanotube (SWNT) using real space tight–binding Hamiltonian to calculate the polarization of the tube electrons. The response function is calculated using standard linear response theory. It is understood that this approach may lead to unpredictable errors in case of the very strong electric fields. In order to take into accounts effects of the modification of the bandstructure of the SWNT we performed special study on what is the action of strong transverse electric field on the density of states (DoS) of the SWNT. In general, for electric fields which are less than typical atomic fields we expect triple effect of the external field on the bandstructure: band shifting, splitting and mixing. We will show that the first effect can be interpreted as a charge injection in the SWNT. The second is related to the symmetry breaking, and the last one is about the polarization of the electron density in the transverse field.

Another important quantum effect that may break the results of the one–electron theory is a Coulomb interaction between electron and hole or an excitonic effect. A few authors attacked this problem recently from different sides. We report here on one aspect of the SWNT exciton theory: selfconsistent study of the screened

Coulomb interaction via an effective dielectric function of the nanotube. This approach fully takes in account the nanotube depolarization.

All of these effects can be useful to control electronic transport through the nanotube channel by optical means. The optical control may be interesting for certain device applications, including optoelectronic devices, for example, opto–electrical switches. We note here that a standard approach to fabricating electrical switch controlled by (quasi–static) external field, or in other words, a field–effect transistor, requires the micro– (nano)–fabrication of an electric gate which applies the potential to the channel. The gate fabrication is tricky as the size scale of the gate should be comparable with the transverse size of the channel (about 1 nm). We proposed recently the use of molecular gates for controlling electronic transport in SWNT transistors.[4–6] The molecule of special structure (as detailed below) can perform the transistor action by absorbing light and changing its mechanical conformation. The change of the electronic properties of the SWNT–molecule complex associated with this mechanical transformation may be strong enough to suppress the charge transport through the channel. Similarly the gating of the ion/molecular/macromolecular flow through the 1D channel can be realized with the proper choice of the molecular gate. Simulation of this device essentially requires the knowledge of the selfconsistent dielectric function of the SWNT.

These three main topics, unified by using the quantum mechanical formalism of the SWNT dielectric function, will be considered below in details.

2. FORMALISM OF SWNT DIELECTRIC FUNCTION: LONGITUDINAL AND TRANSVERSE PHOTONS

This section presents the linear response theory for interaction of the longitudinal and transverse electric fields with the electronic subsystem of the SWNT. The interaction of the longitudinal field has been considered in earlier publications.[7–9] We note that for a typical nanometer size of the system one can safely neglect the retardation effects in the linear response theory of the SWNTs, thus returning to a quasi–static approximation. We adopt this approach here.

We start with the role of the selfconsistent dielectric function in modelling of excitonic correction in the optical response of the SWNTs.

2.1. Selfconsistent depolarization and exciton binding energy in SWNTs

It is worth to note that in 1D systems, for example, in carbon nanotubes, an exciton binding energy is large, diverging with the inverse radius. This is because the Coulomb interaction has a logarithmic singularity in 1D[10] due to a poor screening. When the screening is weak a specific spatial dispersion of a dielectric function must be written. The screening is strong at the distances less than the nanotube radius and is ineffective at the large distances. Actually, the dielectric function of 1D system with zero angular momentum approaches unity in the long wavelength limit.

From the other hand, the *frequency* dispersion of the dielectric function is important as well. This is due to the Coulomb energy and the kinetic energy of the electron in SWNTs scale in the same way. Their ratio is a constant, proportional the 1D density of states (or quantum capacitance of the nanotube, as it will be shown in the Section 3.1). If one considers the numerical value of this constant, one finds that the semiconductor SWNT bandstructure should be unstable with respect to Coulomb perturbations and suffer on the transition into an excitonic insulator. Of course, this picture is wrong and the physical reason is following: although the screening of the valence electrons of the SWNT is weak it has a frequency dependence. As usual when approaching the energy of a typical optical transition, the dielectric function has a peak. The strength of this peak in 1D system is increased because the 1D DoS has a singularity at the edge of the conduction and valence bands. The dielectric function, thus, diverges (when neglecting an absorption or an imaginary part of the dielectric function) and screens the Coulomb potential. This qualitative argument is quantitatively considered below in details.

The key to the problem of selfconsistent calculation of the exciton energy is in solving Bethe–Salpeter equation. We write it as a Scroedinger equation in k–space for the wavefunction of the exciton Ψ_k. For the semiconductor SWNT it reads as[11]:

$$\frac{\hbar^2 k^2}{2\mu^*} \, \Psi_k - \int dq \frac{V_{q,\,0}}{\varepsilon_{q,0}\,(E_b/\hbar)} \, \Psi_{k-q} = -E_b \Psi_k \tag{1}$$
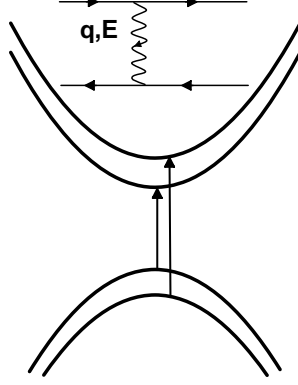
Figure 1. Scheme of electron–hole transitions corresponding to calculated exciton levels. Inset: Feynman diagram corresponding to the exciton state. The interaction line is screened by $\varepsilon_q(E)$.

where $V_{q,0}$ is the Fourier component of a bare Coulomb potential (for optical transition across the gap the angular momentum is conserved, thus the potential $V_{q,m}$ is taken at $m = 0$), $\varepsilon_{q,0}(\omega)$ is the frequency dependent dielectric function at the wavenumber q and angular momentum $m = 0$ ($\varepsilon_q(\omega)$ corresponds to the polarization operator in the RPA–E approximation), $E_b > 0$ and μ^* are the exciton binding energy and a reduced mass, respectively. The reduced mass depends on the nanotube radius as follows:

$$\mu^* = m^*/2 = \frac{\hbar^2}{9bR\gamma_0} = \frac{\hbar^2}{9E_g R^2} \tag{2}$$

taking into account that the SWNT energy gap is

$$E_g = \gamma_0 b/R. \tag{3}$$

Here $b \simeq 1.4\text{Å}$ is the interatomic distance, $\gamma \simeq 2.7$ eV is the hopping integral.

We assume that the electron and the hole are in subbands that are separated by a minimum energy gap. The Fourier transform of the Coulomb potential is given by[12]

$$V_{q,m} = 2e^2 I_{|m|}(|qR|) \, K_{|m|}(|qR|) \tag{4}$$

where $I_m(x)$ and $K_m(x)$ are Bessel functions of imaginary argument.[14] We neglect the Coulomb matrix elements with a nonzero angular momentum in the calculation of the exciton binding energy, which is equivalent neglecting an intersubband mixing as it will be further discussed later on. This approximation is valid due to the small values of these Coulomb matrix elements and sufficiently large distance between subbands (Fig.1). The coupling of the excitons in different subbands can be taken into account in the second-order perturbation theory.

The (longitudinal) dielectric function $\varepsilon_{q,m}(\omega)$ can be written as

$$\varepsilon_{q,m}(\omega) = 1 + \frac{2\,e^2}{\pi} \, I_{|m|}(|qR|) \, K_{|m|}(|qR|) \times \tag{5}$$

$$\sum_{\alpha,\beta=c,v;\ n} \int dk \frac{|\langle k+q, n+m, \alpha | e^{iqz} e^{im\phi} | k, n, \beta \rangle|^2}{E_{k+q,n+m,\alpha} - E_{k,n,\beta} - \hbar\omega} \left(f\left(E_{k,n,\beta} - E_F\right) - f\left(E_{k+q,m+n,\alpha} - E_F\right) \right)$$

where $|k, n, \alpha\rangle$ denotes the state of the conduction/valence band, $\alpha = c/v$, with a longitudinal momentum $\hbar k$ and the angular momentum $\hbar n$; $f(E - E_F)$ is a Fermi distribution function. It was pointed above, that we are interested in the dielectric function with the zero angular momentum, thus, $m = 0$ in the rest of paper.

In vicinity of the one–electron gap, where optical transitions happen and the dielectric function has a singularity, it can be further simplified and reduced to the analytical expression

$$\varepsilon_{q,0}(\omega) = 1 + \frac{8e^2}{\pi b \gamma_0} \frac{3\pi}{4\sqrt{2}} \frac{1}{\sqrt{1-\Omega}} q^2 R^2 \, I_0(|qR|) \, K_0(|qR|) \,, \qquad 1 - \Omega \ll 1 \tag{6}$$

where $\Omega = \hbar\omega/E_g$ is the dimensionless frequency.

Substituting (2) in (1) and introducing the dimensionless wavevector $\tilde{q} = qR$, we obtain a universal equation with no explicit dependence on the nanotube radius

$$\frac{9}{2} \tilde{k}^2 \Psi_{\tilde{k}} - \frac{e^2}{b\gamma_0} \int d\tilde{q} \frac{2I_0(\tilde{q})K_0(\tilde{q})}{1 + \frac{9\pi}{4\sqrt{2}} C_Q \, A \, (E_b/E_g) \, \tilde{q}^2 I_0(\tilde{q}) K_0(\tilde{q})} \Psi_{\tilde{k}-\tilde{q}} = -\frac{E_b}{E_g} \Psi_{\tilde{k}}, \tag{7}$$

where $C_Q = 8e^2/(3\pi b\gamma)$ is the quantum capacitance (see also Section 3.1), and $A(\Omega)$ is the frequency-dependent part of the dielectric function. This equation has been solved in Ref.[11] where further details can be found.

In the calculations with the static dielectric function, the exciton binding energy exceeds the SWNT energy gap due to the weak screening of the longitudinal electric field in 1D systems. In fact, when taking into account space and frequency dispersion of the dielectric function, the exciton binding energy can not be larger than the energy gap (no transition to the excitonic insulator) due to the singularity of the dielectric function at $\hbar\omega = E_g$. Self-consistent calculation of the exciton binding energy with the frequency-dependent dielectric function also showed that the ratio of the exciton binding energy to the energy gap and the ratio of the exciton characteristic length to the nanotube radius are independent on the nanotube radius within the model.

2.2. Transverse dielectric function

The interaction of the SWNT electrons with the transverse photons can be written in a similar way via the dielectric function. We write an induced polarization $P(\mathbf{r})$ of the SWNT in Fourier components in cylindrical coordinates:

$$\mathbf{P}(\mathbf{r}) = \int dk_z \sum_m \mathbf{P}(k_z, m) e^{ik_z z + im\theta}. \tag{8}$$

We note that it has no component normal to the nanotube sidewall because of one–band approximation accepted through the paper. Which means that we neglect transitions between pi and sigma electron bands. The polarization depends on the external field, written in the same cylindrical gauge, via the susceptibility tensor $\chi(k, m)$:

$$P_\mu(k, m) = \chi_{\mu\nu}(k, m)\mathcal{E}_\nu(k, m) \quad \mu, \nu = z, \theta. \tag{9}$$

The dynamic susceptibility $\chi(k, m, \omega)$ of the SWNT within the linear response theory is as follows:

$$\begin{aligned}
\chi_{\mu\nu}(k, m, \omega) &= 2\frac{e^2}{AL} \sum_{m',m''} \sum_{\tau',\tau''=v,c} \int \frac{dk'}{2\pi} \int \frac{dk''}{2\pi} \frac{f\left(E(k', m', \tau') - E_F\right) - f\left(E(k'', m'', \tau'') - E_F\right)}{\left(E(k'', m'', \tau'') - E(k', m', \tau')\right)^2} \\
&\times \frac{\langle k'm'\tau'|j_\mu(k, m)|k''m''\tau''\rangle\langle k''m''\tau''c|j_\nu^+(k, m)|k'm'\tau'\rangle}{E(k'', m'', \tau'') - E(k', m', \tau') - \omega}
\end{aligned} \tag{10}$$

where $E(k, m, \tau)$ is the energy of the electron state with (axial) wavevector k, angular momentum m, and the (conduction/valence) band index $\tau = c, v$. Here L and A are the length and cross section area of the SWNT respectively for normalization purposes.

The current density operator, $\mathbf{j}^+(k, m)$, is closely related to the momentum operator $\mathbf{p}$:

$$\mathbf{j}^+(\mathbf{k}) = \frac{1}{2m_0} \left(e^{i\mathbf{k}\cdot\mathbf{r}}\mathbf{p} + \mathbf{p}e^{i\mathbf{k}\cdot\mathbf{r}}\right) \tag{11}$$

and analytical expression for it, within the tight–binding model, can be found elsewhere.[13]

The expression above becomes useful when the components of the electric field and the polarizability are transformed into the Cartesian coordinates. After some math one can show that, by neglecting small terms proportional to the ratio of the SWNT radius to the light wavelength ($\sim 10^{-3}$), it acquires a simple form:

$$
\begin{aligned}
p_{||}(\mathbf{k}) &= \frac{A}{2}\chi_{\theta\theta}(\mathbf{k},1)\big(J_0(kR) + J_2(kR)\big)\mathcal{E}_{||}(\mathbf{k}) \\
p_{\perp}(\mathbf{k}) &= \frac{A}{2}\chi_{\theta\theta}(\mathbf{k},1)\big(J_0(kR) - J_2(kR)\big)\mathcal{E}_{\perp}(\mathbf{k}) \\
p_z(\mathbf{k}) &= A\chi_{zz}(\mathbf{k},0)J_0(kR)\mathcal{E}_z(\mathbf{k}).
\end{aligned}
\tag{12}
$$

Here $J_m(x)$ are Bessel functions of the order m.[14]

The expression for the transverse dielectric function Eq.(12) is obtained in neglecting the spatial dispersion, which means that we consider the long wavelength limit when derived this formula. However, this holds since the typical transition frequency is in the range of near–IR — visible light and, thus, corresponding wavelength is in the (sub–)micrometer region (to be compared with the SWNT diameter about a nanometer). We use the transverse dielectric function for studying optical response of the SWNT near field probes (to be published elsewhere[15]).

3. BANDSTRUCTURE ENGINEERING IN SWNT

As we discussed in the introduction, applying too strong electric field one can modulate the response of the nanotube beyond "rigid band" approximation. In this section we study the effect of the external electric field on the bandstructure of SWNTs of different symmetry (chirality). As before we neglect the retardation and, moreover, we skip the spatial dependence of the external field as the wavelength of the optical photon is much larger than the radius of the nanotube (~ 1 nm) and the unit cell length (~ 0.3 nm for achiral SWNTs). That means we use an approximation of the quasi–static transverse uniform field through this section. In case of slowly varying electric field of the optical probe it seems to be justified but in case of an electric potential of a local type a special study is required which has to take into account a breaking both transverse and longitudinal symmetry. The effect of the periodicity of the potential *along* the SWNT axis is easy to understand: the periodic potential creates minibands separated by minigaps of forbidden energies (to be published elsewhere). The effect of the breaking the nanotube symmetry in *circumferential* direction is less trivial: there is a finite mixing (and possible splitting) of the subbands of the SWNT in the external transverse field. This may be related to a (non–linear) Stark effect for non degenerate levels, although, we use different formalism of a direct perturbation series expansion. We consider the case when the Stark energy of the field is comparable with the separation between the subbands (the optical band gap) but smaller than the full width of the valence bands (or/and an atomic energy). This allows us using the wavefunctions of the bare Hamiltonian for both analytical and numerical computations.

We start discussion of possible bandstructure modification by considering essentially simpler case of a spontaneous symmetry breaking in the SWNT due to charge injection and subsequent polarization near a substrate surface. This example allows us to trace most clearly how (1) the selfconsistency of the electrostatic calculation is reached and that (2) the band mixing can be understood as a nonuniform polarization of the nanotube. The latter is not trivial in case of the single–wall nanotube. It was discussed in literature that the conducting SWNT (metallic or degenerately doped semiconductor SWNT) behaves as a metal cylinder of the radius (approximately) equal to the average radius of the tube. As a consequence, the mathematical results derived earlier for classical metal cylinders were simply transferred to the SWNT case.

There exist at least two main differences between the electrostatics of the SWNT and the corresponding metal cylinder: (1) the finite density of states of the SWNT results in a reduced screening of the electric potentials as it was shown in Refs..[7, 16] (2) Discrete number of levels of the electron quantization in the *circumferential* direction leads to a *finite* polarizability *across* the nanotube. In other words, even if the conducting SWNT behaves like a metal along the tube axis — conducts current and screens the potential, the same SWNT behaves like an insulator (intrinsic semiconductor) with respect to transverse electric potentials. A simplest example of such difference is that the self–capacitance of the metallic cylinder over the conductor plane is $\mathrm{arccosh}^{-1}(2D/R)/2$

but the SWNT self–capacitance is only $\log^{-1}(2D/R)/2$ which intentionally neglects the self–polarization due to the image charge in the conductor. The influence of the image charge in the conductor has to be included through the quantum mechanical computation. We present one possible solution for this problem below.

3.1. SWNT self–polarization and spontaneous symmetry breaking

We consider the nanotube at the surface of (any) substrate where external potential applied such that it shifts the Fermi level (electrochemical potential, if considering non–zero temperatures) and results in the charge injection into (from) the SWNT. The population of the SWNT by external electrons (holes) may happen either through the substrate itself or from other external leads.

There is an expression for the 1D specific charge density of the biased SWNT (*i.e.*, the SWNT where the electrochemical potential μ is, for example, shifted up from the charge neutrality level which is taken as zero in what follows):

$$\rho = \int e\nu(E) \, f(E - \mu(\rho)) \, dE, \tag{13}$$

here $f(E - \mu(\rho))$ is the Fermi distribution function, and $\nu(E)$ is the SWNT density of states. The latter is constant for the metallic SWNT in the region near the charge neutrality level:

$$\nu_M(E) = \frac{C_Q}{e^2} = \frac{8}{3\pi b\gamma}, \tag{14}$$

and is a sum of divergent contributions from different subbands for a semiconductor SWNT:

$$\nu_S(E) = \sum_m C_Q \frac{E}{\sqrt{E^2 - \Delta_m^2}} \theta(E - \Delta_m), \tag{15}$$

here $\theta(x)$ is the Heaviside unit step function, $C_Q = 8e^2/(3\pi b\gamma)$ is the one–dimensional quantum capacitance[7] (C_Q was introduced first time in Ref.[17] for a two–dimensional electron gas).

One can see that this charge density has no dependence on the circumferential coordinate along the SWNT equator. This is because the bare DoS can be obtained by diagonalizing the Hamiltonian with full axial symmetry. Every solution of this Hamiltonian has definite angular momentum m and, thus, the wavefunctions are proportional to $\exp(im\alpha)$. The density matrix is proportional to the product of wavefunctions with momenta m and n: $\hat{\rho}(m, n) \propto \exp(i(m - n)\alpha)$. The charge density, which is given by the diagonal elements of the density matrix, is independent of α: $\rho \equiv \hat{\rho}(m, m) \propto \delta_{m,n}$. Thus, the bare charge density (at arbitrary Fermi level) cannot have any angular dependence (as we noted in the beginning of the section).

The charge density has to be calculated together with the (local) electrochemical potential in a selfconsistent way. The shift of the μ with respect to the equilibrium is related to (a) the external potential φ^{xt}, including the work function difference ΔW if needed, and (b) the induced potential which in turns depends on the ρ:

$$\mu(\rho) = \Delta W - e\varphi^{xt} - e\varphi^{ind}(\rho). \tag{16}$$

The induced potential can be found by solving the Poisson equation but also by integrating the specific charge density with the 1D Green's function of the Coulomb kernel.[16] The 1D Green's function for discussed geometry is readily obtained. In case of the slow variation of the potential along the tube axis (quasi–uniform field approximation), the integration results in the simple expression for the potential (cf. Refs.[7,16]):

$$\varphi^{ind}(\rho) = C_g^{-1} \rho = 2\log(2D/R) \rho, \tag{17}$$

where $C_g = 1/(2\log(2D/R))$ is the classical (geometrical) capacitance.

Solving Eqs.(13,16,17) together we obtain selfconsistent solutions for the charge density for metallic and semiconductor SWNTs (here we neglect the work function difference $\Delta W = 0$):

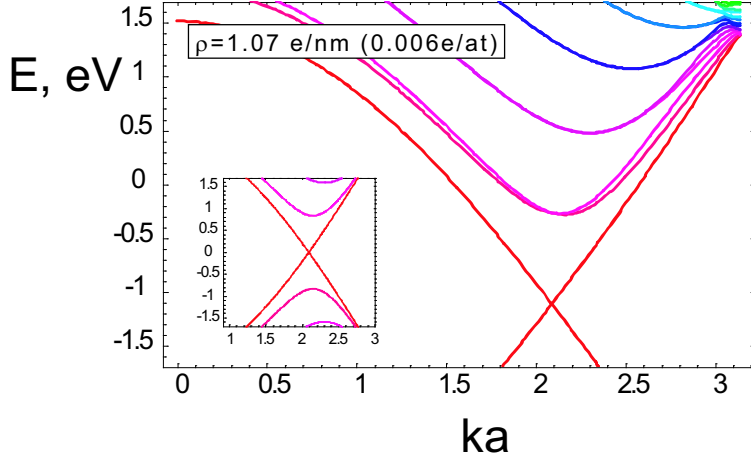$$\rho_M = \frac{-e\varphi^{xt}}{e\left(C_g^{-1} + C_Q^{-1}\right)}, \tag{18}$$

Figure 2. The splitting of the lowest subbands of the [10,10] armchair SWNT due to the substrate polarization at the charge injection $\sim 10^{-2}$ e/atom. Inset: The bare dispersion curves at no charge injected in the SWNT.

and consider that only first subband is filled for the semiconducting SWNT:

$$\rho_S = \frac{-1}{e\left(C_g^{-1} + C_Q^{-1}\right)} \frac{\sqrt{\Delta^2 \left(C_g^{-2} - C_Q^{-2}\right) + \left(e\varphi^{xt}\right)^2 C_Q^{-2}} - C_g^{-1}}{C_g^{-1} - C_Q^{-1}}. \tag{19}$$

We note that this charge density results in the polarization in the substrate which may be represented via an image charge density $\sigma^* = \sigma\frac{1-\varepsilon}{\varepsilon+1}$ where an effective dielectric function of the substrate is ε. For the case of the conductor as a substrate, the image charge is $\sigma^* = -\sigma$. This potential mixes and splits the SWNT subbands. We derived the quantum–mechanical matrix elements between different subbands in Ref.[18] within a tight–binding approximation. The resulting bandstructure is shown in the Fig.2.

3.2. Symmetry breaking and gap opening in quasi–metallic SWNTs

We showed in the last section that the spontaneous breaking of the SWNT band symmetry by the nonuniform field of the polarization charge of the substrate may lead to the essential bandstructure modification in armchair metallic SWNTs. However, it can be explicitly demonstrated with use of a group theory approach that this perturbation cannot open a gap in the armchair nanotube DoS. Thus, the modification of the optical properties is somewhat limited in this case. Although, one can expect strong quasi–Moss–Burstein effect in these materials (to be discussed elsewhere).

Let us consider in this section a case of the quasi–metallic SWNT (for example, zigzag SWNT [3n,0] where n is integer). We will show that this nanotube bandstructure may be effectively controlled by applying external quasi–uniform transverse electric field. The external field perturbs the subbands in a similar way as in the ordinary Stark problem: it mixes subbands with the angular momentum difference $m = \pm 1$ between initial and final states. As a result, the Fermi point of the gapless material may shift in the momentum–energy space. This, in turn, results in the opening of a forbidden gap proportional to the square of the applied field, as for ordinary non–degenerate Stark effect theory. An order of magnitude estimate for the gap may be obtained by equating the dimensionless gap (in units of the hopping integral, γ) to the dimensionless Stark energy (in units of γ):

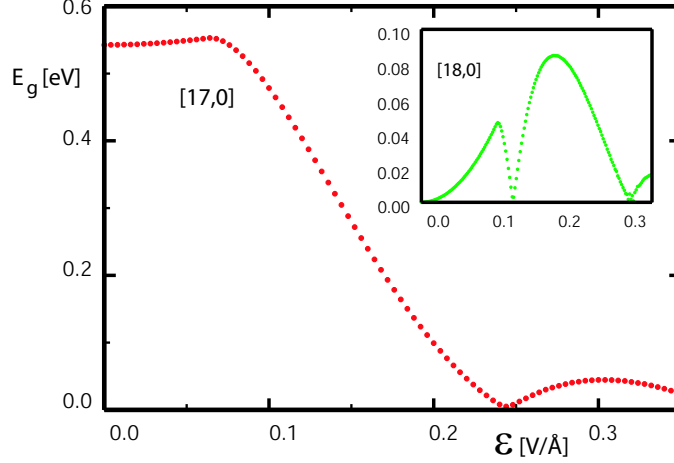$$\frac{E_g}{\gamma} \sim \left(\frac{e\mathcal{E}R}{\gamma}\right)^2, \tag{20}$$

Figure 3. Dependence of the band gap of a [17,0] zigzag nanotube on the field strength. Inset: Same for opening the gap in a [18,0] nanotube.
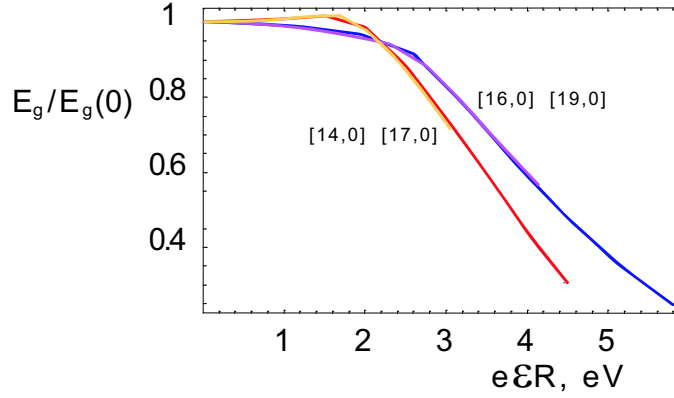

Figure 4. The universal dependence of the gap opening for zigzag SWNTs on the applied electric field. The dimensionless gaps of two classes of SWNTs collapse onto two curves (see text).

where $\mathcal{E}$ is the magnitude of the electric field at the SWNT, R is its radius and e is the electron charge.

The results of the numerical calculation agrees with this expression up to a constant about unity. However, we also found that the gap do not grow constantly but oscillates (see Fig.3). This effect has a simple physical origin: the SWNT has many subbands in the vicinity of the Fermi level. By applying electric field one shifts some of these subbands up and some of them down. Thus, an anticrossing of levels happens for some specific Stark energies. Let us estimate the Stark energy at this the first anticrossing may happen — this will correspond to the first minimum of the otherwise growing forbidden gap. The Stark energy, $e\mathcal{E}R$, should be about the energy distance between subbands. For the SWNTs this energy distance is determined by a space quantization along the nanotube equator and is given by a unique parameter, depending only on the SWNT radius: $\gamma b/R$. This requires that the critical field (at which the first minimum of the gap happens) will be inverse quadratic function of the SWNT radius. Indeed, this scaling of the critical field was obtained in numerical study.

We conclude this section by noting that in a similar way the bandstructure of the semiconducting SWNT may be engineered. The electric field shifts the Fermi point towards the middle of the gap, thus, the gap closing, proportional to the electric field happens. If one normalizes the field dependent band gap of the SWNT, which also depends on the SWNT radius, to the band gap at zero field: $E_g(\mathcal{E})/E_g(\mathcal{E}=0)$ and plot it as a function of the Stark energy $e\mathcal{E}R$, all curves for SWNTs of specific symmetry collapse. We know two types of semiconductor
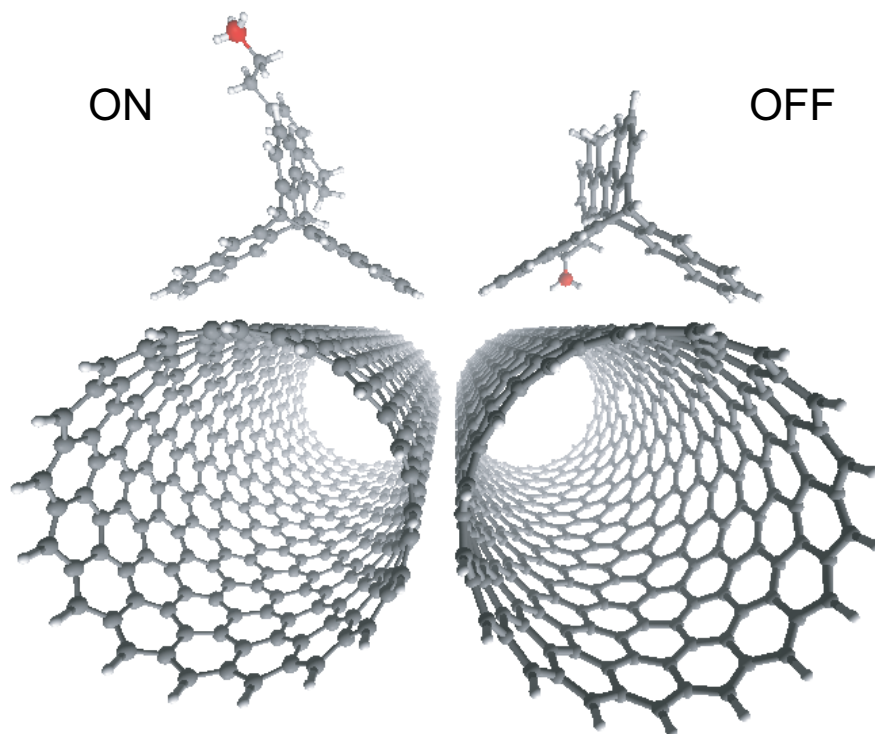
Figure 5. The optimized geometry of the LOMES in ON and OFF states.

SWNTs: [3n+1,0] and [3n-1,0]. The gap dependence on the applied field for these SWNTs is shown in the Fig.4. The minimum of the gap is situated at different sides of the Fermi point for these two types of nanotubes. One can see that at low fields the action of the field is the same for both types of SWNTs — it simply shifts the Fermi point. Thus, the gap slightly decreases (increases) for the given nanotube symmetry when the minimum of the gap is shifting toward (outward) the Fermi point. For larger fields, the anticrossing of the valence and conduction bands plays the major role, so the gap decreases in both types of nanotubes.

4. LIGHT–OPERATED MOLECULAR ELECTRONIC SWITCHES WITH SWNTS

The last section of the paper deals with a complex of an organic molecule and the SWNT. This is an example of the molecular device assembled with a bottom–up fabrication approach (in contrast to a standard top–down approach of semiconductor technology). It would be extremely difficult to make man–made structures of the size scale comparable with the width of the SWNT channel to work as electric gates for transistor switching. It is very appealing to use self–assembled or synthetically grown structures for this purpose. Our approach is in designing a special organic molecule which can perform transistor action, from one side, and will be able to self–assemble with the SWNT channel, from the other side.

To start with we define the required properties of a switching molecule to be useful for electronic switch applications.

(1) The molecule has to be able to absorb at the sidewall of the ideal, defect free, SWNT, presumably, from vapor or solid phase as it will be explained below. The covalent chemistry at the sidewalls of nanotubes, which is rapidly growing area nowadays, may not be fully applicable for the goal of fabricating devices with ultimate performance. Such device should have ideally no scattering at all (ballistic transport) which requires as clean lattice as possible. The SWNT is a great candidate for fabricating ballistic devices because all its sidewall surface has saturated chemical bonds. Breaking these bonds allows creating covalent anchors to the SWNT but
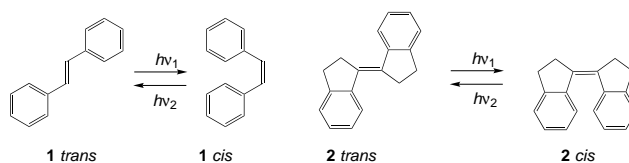
Figure 6. Resonant optical absorption leads to a conformational changes in these "molecular motors"[21,22]: stilbene (**1**) and 1,1'-biindanylidene (**2**). Note that **2** has no single bonds next to the switching double bond in the center of the molecule, thus, has no extra rotational degree of freedom.

also inevitably degrades the performance. Thus, we have chosen the molecule to be attached to the sidewall by non–covalent bonds. The most appropriate non–covalent bonding is van der Waals (or $\pi - \pi$) interaction, because the nanotube can be considered as a large aromatic molecule, having strong interaction to phenol–like rings. Such an attachment would greatly reduce the modification of the electronic structure of the nanotube. Hence, the ideal van der Waals anchor does not change the performance of the device at all.

(2) There may be different ways to modulate the transport through the SWNT. In this paper we propose using the simplest though most effective approach: to control the transport by a local field of the electric charge. Thus, the molecule we design must have a charge moiety. The charged part of the molecule has to be able to move between two mechanically stable positions: far and near the nanotube surface, thus, modulating the potential seen by the transport electrons in the SWNT channel. The charge will be partially screened by the valence electrons of the SWNT channel, which effect we will take into account in a selfconsistent way, similarly to the one described earlier. If the assembly would happen in the wet condition, the charge may also attract counter ions from the solvent. That is why we propose using vapor or dry deposition with pre/post–ionization to obtain charged molecules at the surface of the SWNT without other contaminants. It is also possible to place a strong dipole instead of the point charge to control the transport through the channel. Both potentials will be presented in modelling below.

(3) The most important for the molecule design is the choice of a mechanism of mechanical switching. It is dictated by the balance between the speed of device switching ON and OFF, and the stability of the ON/OFF states. The charged part of the molecule cannot be too flexible to prevent random ON/OFF switching due to the thermal motion, but it cannot be too rigid because then the energy required for switching will be too large and large–scale device integration will meet the problem of energy dissipation.

Many of switching mechanisms, although very robust, require chemical reduction of the molecules and, thus, a typical switching time will be limited by diffusion in the solvent. This rules out using of such mechanism for fast switches operating in a wide range of temperatures and other conditions.

We propose to use the resonant optical absorption for configurational transformations of the designed molecule to fabricate the Light–Operated Molecular Electronic Switch (LOMES).

Recently, a number of reports describing a non-covalent modification of SWNT surface based on $\pi - \pi$ interactions of electron-rich aromatic molecules with the nanotube have appeared.[19] For the proposed LOMES device, in addition to providing the desired $\pi - \pi$ interaction, an aromatic "anchor" of the molecule should provide a geometry suitable for the attachment of a charged moiety (such as a substituted ammonium cation, for example) in a way that places it in the near proximity of the SWNT surface. A bicylcic aromatic system (see below) has been selected to function as the anchor in the LOMES device.

Several classes of molecular switches based on photochromic behavior, optical control of chirality, fluorescence, intersystem crossing, electrochemically and photochemically induced changes in liquid crystals, thin films, membranes, and photoinduced electron and energy transfer have been reported.[20,21] The fastest of the molecular switching processes are intramolecular and intermolecular electron and energy transfer, and *cis/trans* isomerization of stilbenes **1**[21] and similar molecules appeared a suitable switching mechanism. However, additional rotation around single bonds of stilbenes makes their use in a LOMES device questionable, therefore, rigid 1,1'-biindanylidene **2** ("stiff stilbene")[22] was selected for the switching part of the charged molecule.

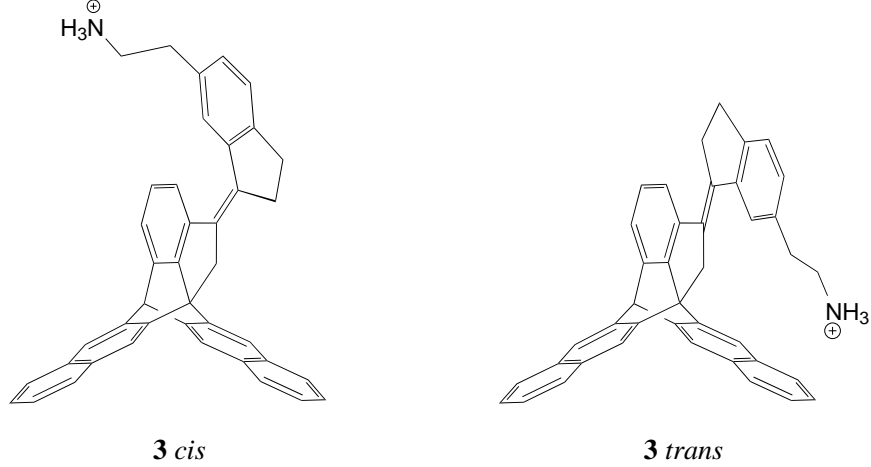**3** *cis*   **3** *trans*

Figure 7.

After combining the components described above, we propose the structure **3** as a prototype switching molecule. It incorporates the bicyclic aromatic anchor suitable for non-covalent attachment to the nanotube surface, with the photoswitchable **2** unit carrying a charged ethylammonium moiety. The ON (*cis*) and OFF (*trans*) states in **3** can be interconverted by irradiation with UV light of 352 nm and 340 nm wavelength,[22, 23] respectively, and switching time will be on the order of 1 – 60 ps.[24] The "tail" of the molecular switch has been chosen to bear a positive charge because we propose its use for modulating the transport in the p–doped nanotubes.

4.1. Selfconsistent potential of the point charge

The electrostatic potential of the point charge near the nanotube surface depends on its position relative to the tube axis. An equilibrium radial distance to the axis of the SWNT, ρ, has been obtained with a quantum chemical calculation in[4] and constitutes ~ 1.2 nm. In cylindrical coordinates, the potential reads as follows:

$$\phi_{xt}(z, \beta, \rho) = \frac{q}{\sqrt{R^2 + \rho^2 + z^2 - 2R\rho \cos \beta}}, \tag{21}$$

where ρ is the cylindrical coordinate of the charge q, z, R and β are the coordinates of the electron (the longitudinal distance to the charge, the nanotube radius and the angular coordinate).

The local band bending is due to the local shift of the bandstructure of the SWNT by this electrical potential. The quantum mechanical description of this mechanism is presented elsewhere.[18] In neglecting the mixing between subbands (that was considered in the last section for stronger fields), which means a conservation of an angular momentum of the electron , $\delta m = 0$, only the component of the electric potential with the full axial symmetry is considered. Thus, the above expression has to be integrated over the β. The amplitude of the potential is given by a prefactor q/R:

$$\phi_{xt} = \frac{q}{R} \mathcal{F}\left(\frac{z}{R}, \frac{\rho}{R}\right), \tag{22}$$

which has to be multiplied by a dimensionless integral $\mathcal{F}$

$$\mathcal{F} = \int_0^{2\pi} \frac{d\beta}{\sqrt{(z/R)^2 + 1 + (\rho/R)^2 - 2 \cos \beta \, \rho/R}} =$$

$$\frac{4}{\sqrt{(z/R)^2 + (\rho/R - 1)^2}} \, K\left(-\frac{4\rho R}{z^2 + (\rho - R)^2}\right). \tag{23}$$

Here K is a complete elliptic integral of the first kind.[14] The integral depends on the dimensionless longitudinal distance to the charge, z/R, and on the ratio of the radial coordinates of the charge and the electron, ρ/R, as a parameter. The latter is about 1.7 for a typical complex.

An expansion of the potential in series in z near the maximum gives only even powers of the distance, thus, at small distances it is a parabolic potential barrier or well, depending on the signs of the external charge, q, and of the major charge carriers in the nanotube, e.

When $eq > 0$ the transport of charge carriers through the SWNT channel will be impeded by the switching molecule. In order to calculate the corresponding current–voltage curves (IVCs), we calculate the transmission probability for the charge carrier of given energy and, then, integrate it over energy with the Fermi distribution function.

So far, the potential was not selfconsistent. The selfconsistency, in the same sense as in RPA–E approximation, can be achieved by summing up all "bubble" diagrams for interaction of the valence electron (hole) in the channel of the SWNT with the charge of the switching molecule. A simpler semiclassical description for the electrostatics of nanotubes has been developed in Ref.[5] and uses the dielectric function formalism and the distributed atomistic capacitance as described in Sec.3.1. Within this formalism we obtain the selfconsistent electric potential by dividing the external potential by a depolarization factor smaller than unity:

$$\phi_{act} = \frac{C_Q^{-1}}{C_g^{-1} + C_Q^{-1}}\phi_{xt} \simeq \phi_{xt}\,\frac{C_Q^{-1}}{C_g^{-1}} \tag{24}$$

here we used same notations $C_g^{-1} = 2\log\left(\frac{L}{R}\right)$ and $C_Q \sim 3.2$ for the geometrical and quantum capacitance. The characteristic length L is given by the smallest distance to the closest conductor. Because this length is placed under the logarithm sign, the resulting depolarization factor changes only slightly and is in the range of $0.02 - 0.04$ for almost any typical SWNT device.

Besides the depolarization due to the electrons in the SWNT we have to take into account the substrate depolarization. We propose the same image charge method as before to take into account the latter. This adds an extra term to the potential in Eq.(21) and Eq.(22)

$$\frac{q^*}{\sqrt{R^2 + \rho^2 + 4h\rho\sin\beta + 4h\rho^2 + z^2}}, \tag{25}$$

where q^* is the image charge of the molecule in the substrate. The latter is given by a simple relation:

$$q^* = q\frac{1-\varepsilon}{\varepsilon+1}, \tag{26}$$

where ε is the dielectric function of the substrate. For typical values of $\varepsilon \sim 12$ for Si, we consider $q^* \simeq -q$, like for metals.

The total potential depends on the angular position of the charge with respect to the substrate and is plotted in Fig.8, Left, for different angular positions.

4.2. Selfconsistent potential of the point dipole

We note that the current through the SWNT channel may be controlled not only by a charged moiety at the free end of the switching molecule but also by a strong dipole placed instead the charge.

The potential created by a single point dipole at the surface of the SWNT depends substantially on the orientation of the dipole with respect to the axis of the nanotube. In the paper we consider the only intra–subband scattering of the charge carriers (with angular momentum conservation), thus, only the longitudinal component of the potential is important. For simplicity we do not consider here the dipole which has all three components being non–zero. In the coordinate system of z–axis pointed along the tube, one perpendicular component of the dipole, p_y, is taken to be zero, which corresponds to the vector of the dipole, $\vec{p}$, staying in the plane with $\vec{z}$. Then, the dipole orientation is given by one variable, α, the angle between the dipole direction
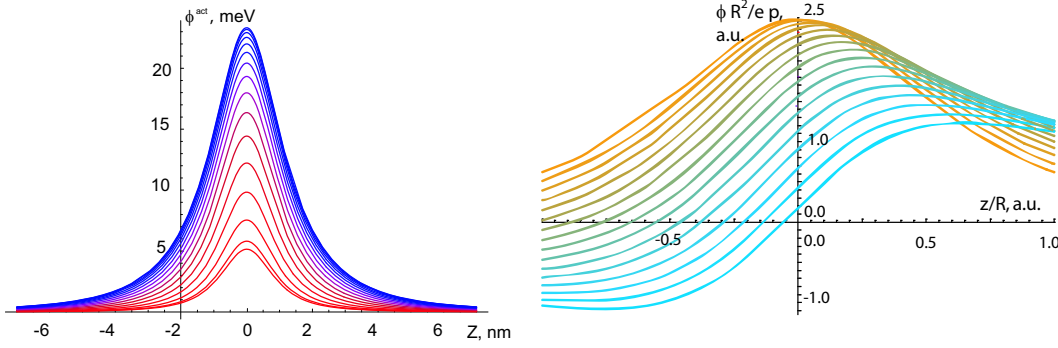
Figure 8. Left: Selfconsistent solution for the electric potential created by a charged impurity along the SWNT axis. Different curves correspond different angular positions of the charge: the maximum potential is for the charge on top of the SWNT. Right: Selfconsistent solution for the one–dimensional electric potential (created by a point dipole) absorbed on the SWNT surface. The color of each curve (from red to blue) corresponds to the angle of the dipole to the tube axis.

and its radial axis, which is chosen as x–axis in this paper. Then, the dipole–electron interaction energy reads as follows:

$$e\phi_{\mathrm{dip}}(z, \beta, \alpha, \rho) = \frac{ep\left((\rho - R\cos\beta)\cos\alpha + z\sin\alpha\right)}{\left(R^2 + \rho^2 + z^2 - 2R\rho\cos\beta\right)^{3/2}}, \tag{27}$$

where R, ρ, β and z have the same definition as in Eq.(21) and $(\pi/2 - \alpha)$ is the angle between the dipole, $\vec{p}$, and the tube axis, $\vec{z}$. Once again, the potential has to be averaged over the electron positions on the tube surface, given by the angle β. As a result one gets a combination of the elliptic functions of z/R multiplied by an amplitude of the potential, which is ep/R^2. In Fig.8, Right, we plot the dimensionless potential (divided by the maximum amplitude) versus the distance along the z–axis, for different dipole orientations.

4.3. Transmission probability

One can easily calculate the transmission through the barriers created for the electrons (holes) by the charge (or dipole) placed close to the SWNT surface. A simple estimate will be given by expanding the acting potential near the maximum and using a semiclassical (WKB) probability for the reflection from the harmonic potential barrier.[25] We obtain the transmission coefficient for a single molecular gate as follows:

$$\mathcal{T}(E) = \frac{1}{1 + \exp\left[-2\pi\frac{E - \varphi(0)}{\hbar}\sqrt{\frac{m^*}{\partial^2\varphi(0)/\partial z^2}}\right]}, \tag{28}$$

where m^* is an effective mass at the band edge, which is given by expression

$$m^* = \hbar^2\left(\frac{\partial^2 E}{\partial k^2}\right)^{-1} = \frac{2\hbar^2}{9bR\gamma}, \tag{29}$$

for the SWNT of the radius R and is about 0.06 of the free electron mass for $R \simeq 0.7$ nm. Here $\gamma \simeq 2.7$ eV is a hopping integral and $b \simeq 0.14$ nm is a SWNT bond length as defined earlier. The transmission coefficient for the potential created by the point dipole is given by a similar expression.

In a ballistic regime, the conductance of the semiconductor SWNT at low voltage can be written as:

$$G = 2G_o\mathcal{T}(E_F) \tag{30}$$

here $2G_o = 2e^2/h$ is four times of the quantum of conductance (because of two spin × two angular momentum channels of the SWNT). Considering the low voltage (linear) regime, the current modulation is given by the modulation of the conductance as in Eq.(30). We present a typical room temperature IV curve of the LOMES
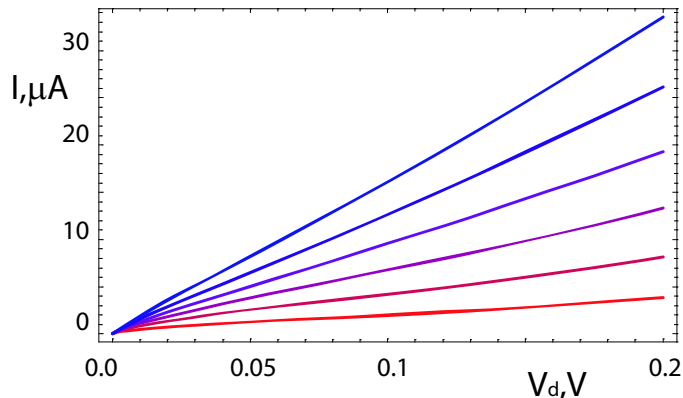
Figure 9. IV curve for a charge scattering. The color of each curve (from red to blue, bottom to top) corresponds to increasing Fermi level from 0.01 to 0.21 eV from the band edge. Parameters of the model are described in the text.

with a semiconductor tube of a radius ~ 0.7 nm and a gap ~ 0.6 eV, degenerately doped (or shifted to this degeneracy by applying the external gate voltage). The IV curves in Figure 9 correspond to the Fermi levels from 0.01 eV (red) to 0.21 eV (blue) from the bottom of the conduction band. For given parameters the amplitude of the barrier, created by the unit charge on the SWNT surface, is ~ 0.26 eV and the barrier width is several nanometers. The IVC has only slight dependence on temperature.

We note that the transmission probability $\mathcal{T}$, and hence, the LOMES conductance is an exponential function of the charge–nanotube distance, ρ. Thus, changing the molecule conformation and the radial coordinate of the charge, ρ, one can effectively modulate the current.

5. CONCLUSIONS

In summary, we presented here a quantum mechanical approach for calculating the dielectric function of single–wall nanotube within tight–binding approximation. The formalism of the dielectric function may serve as a standard method to obtain a selfconsistent solution for numerous problems of SWNT electronics, opto–electronics and nano–photonics. In the paper we presented several examples: from a pure single nanotube in vacuum to a self–assembled molecular device, where the formalism of the dielectric function was a key element of the modelling. A problem of an exciton in the SWNT had suffered of inconsistent treatment of the electron–hole Coulomb interaction which was solved by including the longitudinal dielectric function in the screened Coulomb potential. We also presented the expression for the transverse dielectric function, in neglecting the spatial dispersion, which may be used for calculating optical properties of SWNT probes (to be published elsewhere). The knowledge of the selfconsistent depolarization of the SWNT was used in studying the symmetry breaking and bandstructure modulation of the SWNT in strong electric fields. We demonstrated the possibility of opening the band gap in ordinarily metallic SWNTs and closing the gap in semiconductor SWNTs. Finally, the method was applied to a novel switching device: light–driven molecular switching element. This device consists of the SWNT channel and an attached molecule which has ability to change its conformation (and, thus, the potential applied to the SWNT surface) by absorbing the light of certain wavelength. The formalism of the dielectric function developed in the paper appears to be a very effective theoretical tool both for the studying fundamental physics of SWNTs and nanotube based novel materials and for the simulation of nanoscale devices.

ACKNOWLEDGMENTS

REFERENCES

1. S. Iijima, Nature, **354**, 56, 1991.

2. R. Hillenbrand, F. Keilmann, P. Hanarp and D. S. Sutherland, J. Aizpurua, "Coherent imaging of nanoscale plasmon patterns with a carbon nanotube optical probe", Applied Physics Letters **83**, Issue 2, pp. 368-370, 2003.

3. S. T. Huntington, S. P. Jarvis, "Application of carbon nanotubes to topographical resolution enhancement of tapered fiber scanning near field optical microscopy probes", Review of Scientific Instruments, **74**, Issue 5, pp. 2933-2935, 2003.

4. S.V. Rotkin, I.Zharov, "Nanotube Light-Controlled Electronic Switch", International Journal of Nanoscience **1** (3/4), pp. 347–356, 2002.

5. S.V. Rotkin, I.Zharov, "Conductivity of a SWNT with a Positive Charge at the Surface", in Proceedings – Electrochemical Society, **2002–12**, P.V. Kamat, D.M. Guldi, and K.M. Kadish, Eds.: ECS Inc., Pennington, NJ, USA. pp. 520–529, 2002.

6. S.V. Rotkin, "From Quantum Models to Novel Effects to New Applications: Theory of Nanotube Devices", in *Applied Physics of Nanotubes: Fundamentals of Theory, Optics and Transport Devices*, Nanoscience and Nanotechnology Series, Ser.Ed.: Ph. Avouris, Springer Verlag GmbH Co. KG (2005).

7. K.A. Bulashevich, S.V. Rotkin, "Nanotube Devices: Microscopic Model," JETP Letters 75, pp. 205–209, 2002.

8. S.V. Rotkin, "Theory of Nanotube Nanodevices", in *Nanostructured Materials and Coatings for Biomedical and Sensor Applications*, Editors: Y.G. Gogotsi and Irina V. Uvarova. Kluwer Academic Publishers: Dordrecht-Boston-London. NATO Science Series: II. Mathematics, Physics and Chemistry — Vol. **102**, pp. 257–277, 2003.

9. K.A. Bulashevich, Master thesis (in Russian), St.Petersburg Technical University, Russia. 2003.

10. R. Loudon, Am. J. Phys. **27**, 649, 1959. L.K. Haines, D.H. Roberts, "One-dimensional hydrogen atom", Am. J. Phys. **37** (11), 1145, 1969.

11. K.A. Bulashevich, S.V. Rotkin, R.A. Suris, "Excitons in Single Wall Carbon Nanotubes", International Journal of Nanoscience, vol. **3** (2), in press, Apr 2004.

12. T. Ando, *J. Phys. Soc. Jp.* **66**, 1066, 1997.

13. Y. Li, S.V. Rotkin, U. Ravaioli, and K. Hess, "Gap Engineering in Metal Nanotubes", unpublished.

14. M. Abramovitz and I.A. Stegun, *Handbook of Mathematical Functions.* Dover, New-York, 1964.

15. S.V. Rotkin, Y. Li, and P.S. Carney, "Probe functions in near-field inverse scattering with application to nanotubes", unpublished.

16. S.V. Rotkin, V. Shrivastava, K.A. Bulashevich, and N.R. Aluru, "Atomistic Capacitance of a Nanotube Electromechanical Device", International Journal of Nanoscience vol. **1**, No. 3/4, pp. 337–346, 2002.

17. S. Luryi, "Quantum capacitance devices", Appl. Phys. Lett. **52** (6), pp. 501–503, 1988.

18. A.G.Petrov, S.V.Rotkin, "Breaking of Nanotube Symmetry by Substrate Polarization", Nano Letters, **3** (6), pp. 701–705, 2003.

19. J. Kong, H. Dai, J. Phys. Chem. B. **105**, 2890, 2001.

20. Molecular Machines Special Issue. Acc. Chem. Res. 2001, 34.

21. Lukas, A. S.; Wasielewski, M. R. Approaches to a molecular switch using photoinduced electron and energy transfer. In *Molecular Switches*, Feringa, B. L., Ed. Wiley-VCH: Weinheim, Germany, 2001, pp. 1–35.

22. Hohlneicher, G.; Wrzal, R.; Lenoir, D.; Frank, R. "Two-Photon Spectra of Stiff Stilbenes: A Contribution to the Assignment of the Low Lying Electronically Excited States of the Stilbene System". Journal of Physical Chemistry A **103**(45), pp. 8969–8975, 1999.

23. Gudipati, M. S.; Maus, M.; Daverkausen, J.; Hohlneicher, G.; Chem. Phys. **192**, 37, 1995; and references therein.

24. Waldeck, D. H. Chem. Rev. **91**, 415–436, 1991.

25. L.D. Landau, E.M. Lifshits. *Quantum Mechanics*, Pergamon, Oxford, 1984.